EXTENDING THE IMAGE RESOLUTION OF ANIMAL PET VIA ACCESSORY INSERT DEVICES

Yuan-Chuan Tai, Heyu Wu, Debashish Pal, Joseph A. O'Sullivan

Washington University in St. Louis, St. Louis, Missouri, USA

ABSTRACT

We have developed two prototype micro insert devices based on a novel virtual-pinhole PET geometry. These devices can be integrated into an animal PET scanner to significantly enhance its image resolution. The first system consists of a rotation stage that rotates a high-resolution detector module within the animal port. The second system consists of 18 detector modules arranged in a ring. While both systems are capable of higher resolution PET imaging, the second approach enables dynamic and gated imaging, as well as higher sensitivity. Image reconstruction algorithms that specifically model the virtual-pinhole PET geometry are developed for the PET insert systems. Preliminary imaging experiments show improvement in transverse image resolution. To achieve quantitative accuracy, refined correction techniques for attenuation and scatter, as well as system normalization and detector dead time, will need to be developed for PET insert devices.

Index Terms— animal PET, high resolution imaging, virtual-pinhole PET, PET insert

1. INTRODUCTION

Tremendous progress has been made in high resolution animal PET imaging technologies in the past decade [1-3]. Many research prototypes as well as commercial scanners have made animal PET imaging widely accepted for molecular imaging research and drug development. Recent effort in animal PET techniques has focused on further improving the image resolution and sensitivity of the scanner because (a) sub-millimeter image resolution is highly desirable in order to better image transgenic mice that model human diseases; and (b) sensitivity of a scanner is often the deterministic factor on whether the imaging technique can be used to study a specific biological question. However, it is extremely difficult to achieve both high resolution and high sensitivity at the same time [4, 5]. Therefore, most existing animal PET scanners have a peak sensitivity ranging from 0.5% to 10% and an image resolution ranging from 1.3 mm to 2.2 mm full-width-at-half-maximum (FWHM).

Many research groups continue to develop new types of PET detectors in order to improve one or both aspects of PET scanners. However, almost all existing effort employs conventional PET system geometry. That is, identical detectors are arranged into multiple planes or rings to enclose the object to be imaged. Coincidence lines-of-response between these identical detectors have the highest resolution at the center. Therefore, the object is often centered in the gantry. We took a different approach and proposed a virtual-pinhole (VP) PET geometry that combines high-resolution and low-resolution detectors in a system to achieve high-resolution images [6]. Through this geometry, we have developed high-resolution insert devices that can be integrated into an existing animal PET scanner to further improve its image resolution. This paper describes the theory of operation of PET insert devices and the initial performance of two prototype insert systems.

2. METHODS

A VP-PET system consists of a group of high-resolution detectors in coincidence with a group of low-resolution detectors. Coincidence lines-of-response between a high-resolution detector element and the entire array of the low-resolution detectors form a cone beam geometry that is similar to what is found in a SPECT system using a pinhole collimator. If the object being imaged is positioned near the high-resolution detectors, the intrinsic spatial resolution of the coincidence lines-of-response sampling the object is predominantly determined by the width of the high-resolution detectors and is less sensitive to the width of the low-resolution detectors. This is an analogy to the pinhole SPECT system where the image resolution is predominantly determined by the aperture size of the pinhole instead of the intrinsic spatial resolution of a gamma camera.

Based on this geometry, we have studied the potential of using high-resolution PET detectors as an accessory insert device to improve the image resolution of animal PET. Figure 1 illustrates the VP-PET geometry formed by a simple PET insert device that consists of a high-resolution PET detector inside a full-ring PET scanner. By rotating the insert detector around the object being imaged, high-resolution tomographic images of the radiotracer distribution within the object can be obtained.

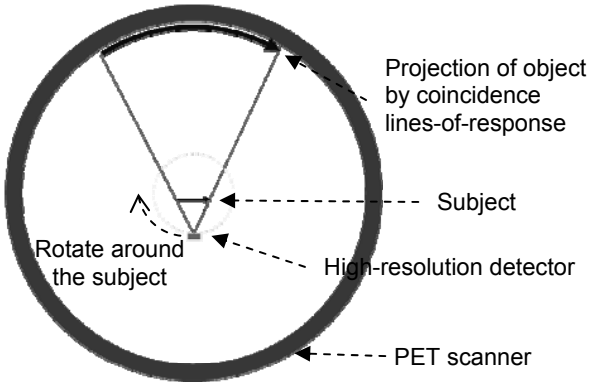

Figure 1. VP-PET geometry can be formed by a high-resolution insert detector inside a PET scanner. Coincident events between the insert and the scanner collected at different angles permit tomographic images to be reconstructed with high resolution.

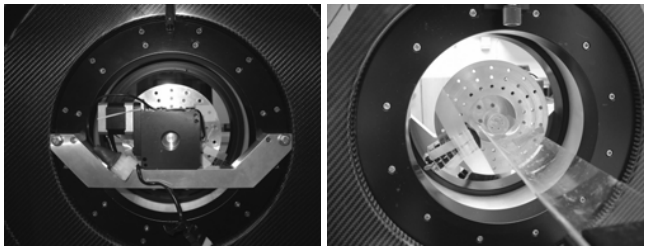

Figure 2. Single-detector prototype micro insert system mounted in microPET F-220 scanner. L: back view. R: front view.

2.1. Single-detector prototype micro insert system

We recently developed the first prototype micro insert device [7] that can be attached to a microPET F-220 system [8] (Siemens Molecular Imaging, Knoxville, TN, USA) to provide higher resolution for mouse imaging. This device consists of a high-resolution detector array, a rotation stage, a custom mounting bracket, and a control PC (shown in Figure 2 without the control PC). The detector consists of a 12 x 24 LSO crystal array. Each crystal measures 0.8 x 0.8 x 3.75 mm^3 with a pitch of 0.86 mm in both directions. The LSO array is directly coupled to a position-sensitive (PS) PMT (R5900-C12, Hamamatsu Photonics, Japan) using the same readout circuits that are used in the microPET F-220. The detector module is mounted on a rotation stage which can be attached to the scanner via a custom mounting bracket after removing the transmission source holder from the scanner. The rotation stage is concentric with the detector rings in the scanner and positioned such that the center of the insert detector block is aligned with the center plane of the second detector ring (out of 4 rings in the scanner). This layout was designed to permit coincidence events between the insert detector and the detector rings #1, #2 and #3 in the scanner.

To establish coincidence detection, an original detector module in ring #4 was unplugged from its electronics. Signals from the high-resolution insert detector are fed into this electronic channel. Crystal lookup table was created by grouping 2 adjacent 0.8 x 0.8 x 3.75 mm^3 LSO crystals into one pseudo-crystal of 0.8 x 1.66 x 3.75 mm^3 so that the LSO array has 12 x 12 pseudo-crystals. After the lookup table and photopeak information are loaded into the scanner, coincidence events between the insert and the microPET scanner can be extracted from the list mode data file.

Figure 3. Full-ring prototype micro insert system mounted in microPET F-220 scanner. L: back view. R: front view.

To image an object, the control PC first rotates the insert detector to an initial angle then issues a command to the microPET host PC to start data acquisition. Subsequently, the control PC rotates the insert detector to a new angle and repeats the data acquisition with the acquisition time adjusted for decay of radioactivity. This step-and-collect procedure is repeated for 9 times to provide 180° sampling of the object. List mode data files are processed by a custom sorting program to create 2D fan beam sinograms using single slice rebinning algorithm [9] or fully 3D cone beam sinograms. We have developed two types of reconstruction algorithms that model the VP-PET geometry used by this prototype system [10]. The first algorithm only works on the 2D fan beam sinogram and is based on filtered-backprojection method modified from the fourth generation CT geometry. The second algorithm can be applied to both 2D and 3D sinograms and is based on maximum-likelihood expectation-maximization (ML-EM) method.

2.2. A full-ring prototype micro insert system

We developed a second prototype micro insert system that consists of 18 high-resolution detector modules arranged into a single ring of 55 mm in diameter. Each detector module consists of a 12 x 12 LSO crystal array, a plastic fiber bundle, and a PS-PMT (R5900-C12, Hamamatsu Photonics, Japan). Each crystal measures 0.74 x 1.54 x 3.75 mm^3 with a pitch of 0.8 mm in the transverse direction and 1.6 mm in the axial direction. That is, the crystal pitch remains the same as the original microPET F-220 scanner in the axial direction, but is reduced by 50% in the transverse direction to improve the in-plane image resolution. The use of fiber bundle is to direct the scintillation light to PS-PMT that are placed outside of the axial field of view so that the gamma ray signals will not be attenuated by the PS-PMT. All detector modules are housed by a light-tight enclosure that can be attached to the microPET F-220 scanner after its transmission source holder is removed.

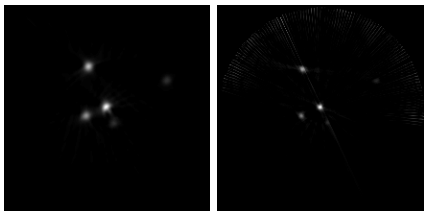

Figure 4. Five capillary tubes filled with ^{18}F-fluoride solution and positioned at 0, 4, 5, 10, 15 mm from the center of field-of-view and imaged by the microPET F-220 scanner (left) and by the single-detector prototype micro insert system (right). The resolution of the original scanner ranges from 1.7 to 2.1 mm FWHM while that of the micro insert ranges from 0.9 to 1.2 mm FWHM.

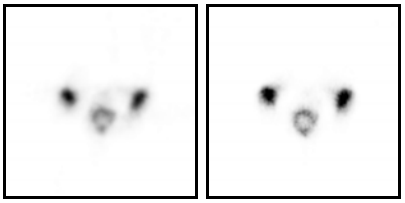

Figure 5. A 23.2 g mouse was injected with 38.5 MBq ^{18}F-fluoride and imaged by the microPET F-220 system (Left) and by the single-detector prototype micro (Right) 3 hours post-injection.

To establish coincidence detection, 18 detector modules in ring #1 of the scanner were unplugged from their electronics. Signals from the 18 insert detectors are fed into these electronic channels. After the crystal lookup tables and photopeak information are set up, coincidence events between the insert and the microPET scanner can be extracted from the list mode data files.

Unlike the first prototype system, this system does not require rotation of the insert detectors. Therefore, no control PC is necessary. An animal can be imaged using the default data acquisition GUI (MicroPET Manager). However, the list mode data needs to be sorted by a custom sorting program to obtain 3 types of sinogram. That is, coincidence events between detectors in the insert (II events), between the insert and scanner (IS events) and between detectors in the original scanner (SS events). The II and SS types of events are similar to those obtained by a conventional animal PET scanner except that the II dataset has a much higher resolution than the SS dataset. The IS type of events are acquired by a VP PET geometry and should provide improved image resolution when compared to the original microPET scanner. The ML-EM algorithm described previously was further modified to combine all 3 types of coincidence events to jointly estimate the images in order to optimize the system sensitivity and image resolution at the same time.

2.3. Initial imaging experiments

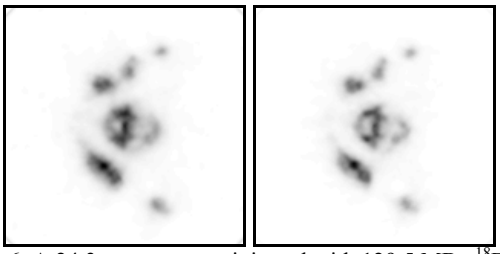

Figure 6. A 24.3 g mouse was injected with 129.5 MBq ^{18}F-fluoride and imaged by the full-ring prototype micro insert device 3.5 hours post-injection. Images were reconstructed using SS type of coincidences alone with resolution similar to that of the original scanner (Left) or using all 3 types of coincidences with improved resolution (Right).

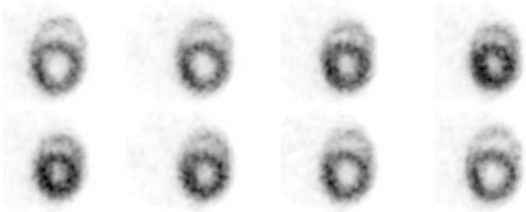

Figure 7. A 22.8 g mouse was imaged by the full-ring prototype micro insert device with EKG gating immediately after a 14.3 MBq ^{18}F-FDG injection. Data were sorted into 8 gates and reconstructed using ML-EM algorithm.

We imaged five ^{18}F-fluoride line sources and skeleton of a mouse after ^{18}F-fluoride injection to demonstrate the resolution improvement using the first prototype system. We also imaged a mouse skeleton with ^{18}F-fluoride using the full-ring prototype system. Gating capability of the full-ring prototype system was tested with a mouse heart study with ^{18}F-FDG injection and EKG gating.

3. RESULTS

Figure 4 shows five ^{18}F-fluoride line sources imaged using the original scanner (Left) and the single-detector micro insert device (Right). The improvement in image resolution near the center of field-of-view can be clearly seen in these images. Figure 5 shows the bone structure of a mouse skull imaged using the original scanner (Left) and the single-detector micro insert device (Right).

Figure 6 shows the bone structure of a mouse spine imaged using the original scanner (Left) and the full-ring prototype micro insert device using all three types of coincidence events (Right). Image from the Figure 7 shows a mouse heart at different phases of a cardiac cycle imaged with the full-ring prototype system. The improvement in image resolution allows us to delineate left and right ventricles clearly.

4. DISCUSSIONS

The two prototype systems shown in this work were both designed to retrofit into an existing animal PET scanner. This approach imposes a number of restrictions to the detector and system design and prohibits us from developing an insert device with the best performance. For example, in order to read the insert detectors using existing electronics in the scanner, the number of crystals in each detector block is limited to 144 (12 x 12). To maintain a reasonable axial image field-of-view, we chose to keep the axial crystal pitch of the insert detector to be approximately the same as that of the scanner and only reduce the transverse crystal pitch of the insert detector. The result is that we could only improve the image resolution in the transverse direction (tangential and radial resolutions) but not the axial resolution. If we were able to design an insert system without this restriction, we could have reduced the crystal pitch in both direction and further improve the volumetric image resolution by approximately 50%.

The current implementation of the insert device requires us to remove the transmission source from the scanner, which prohibits the users from performing transmission imaging for attenuation correction. One possible solution is to co-register the emission image with microCT images and use the latter for calculated attenuation correction.

Quantitative accuracy of the micro insert systems has not been fully validated. The presence of insert detectors inside the imaging field-of-view leads to additional scatter and attenuation of the gamma rays. In addition, with the insert device in the path of many coincidence lines of response between detectors in the original scanner, the coincidence detection efficiency of the scanner detectors is significantly affected and becomes less uniform. Furthermore, the insert detectors are positioned very close to the subject and are subject to higher singles rate, which may lead to higher dead time for the insert device. All these factors challenge the quantitative accuracy of PET images using the insert device and will require more sophisticated correction techniques before the micro insert device can be used for routine PET studies.

5. CONCLUSIONS

Through the two prototype micro insert systems, we have demonstrated the feasibility of using accessory insert devices to further improve the image resolution of existing animal PET scanners. This may provide an alternative to the conventional approach that relies on a single type of detector to achieve both high image resolution and high system sensitivity, which has been shown to be technically challenging. The same idea can also be applied to develop insert devices to significantly improve the image resolution of clinical PET scanners. Further investigation is necessary before the full potentials of PET insert technique can be determined.

6. ACKNOWLEDGEMENTS

The authors would like to thank Stefan B. Siegel and Danny F. Newport of Siemens Molecular Imaging, Inc. for their inspiring discussion; and Dennis Tapella, John Kreitler and the staffs of the microPET Lab of Washington University in St. Louis for their technical support. This work was supported in part by the National Cancer Institute of NIH (Grants R24-CA83060 and R33-CA-110011) and by the Susan G. Komen for the Cure (Grant BCTR0601279).

7. REFERENCES

[1] A. F. Chatziioannou, "PET scanners dedicated to molecular imaging of small animal models," *Mol Imaging Biol*, vol. 4, pp. 47-63., 2002.

[2] A. Del Guerra and N. Belcari, "Advances in animal PET scanners," *Quarterly Journal of Nuclear Medicine*, vol. 46, pp. 35-47, 2002.

[3] M. Larobina, A. Brunetti, and M. Salvatore, "Small animal PET: A review of commercially available imaging systems," *Current Medical Imaging Reviews*, vol. 2, pp. 187-192, 2006.

[4] S. R. Cherry, "In vivo molecular and genomic imaging: new challenges for imaging physics," *Physics in Medicine & Biology*, vol. 49, pp. R13-48, 2004.

[5] Y.-C. Tai and R. Laforest, "Instrumentation aspects of animal PET," *Annual Review of Biomedical Engineering*, vol. 7, pp. 255-285, 2005.

[6] Y.-C. Tai, H. Wu, D. Pal, and J. A. O'Sullivan, "Virtual-Pinhole Positron Emission Tomography," *Journal of Nuclear Medicine*, vol. (In Press).

[7] H. Wu, D. Pal, J. A. O'Sullivan, and Y.-C. Tai, "A Feasibility Study of a Prototype PET Insert Device to Convert a General Purpose Animal PET Scanner to Higher Resolution," *Journal of Nuclear Medicine*, vol. 49, pp. 79–87, 2008.

[8] Y.-C. Tai, A. Ruangma, D. Rowland, S. Siegel, D. F. Newport, P. L. Chow, and R. Laforest, "Performance Evaluation of the microPET-Focus: a third generation microPET scanner dedicated to animal imaging," *Journal of Nuclear Medicine*, vol. 46, pp. 455-463, 2005.

[9] M. E. Daube-Witherspoon and G. Muehllehner, "Treatment of axial data in three-dimensional PET," *Journal of Nuclear Medicine*, vol. 28, pp. 1717-24, 1987.

[10] D. Pal, J. A. O'Sullivan, H. Wu, M. Janecek, and Y.-C. Tai, "2D Linear and Iterative Reconstruction Algorithms for a PET-Insert Scanner," *Physics in Medicine and Biology*, vol. 52, pp. 4293-4310, 2007.